# ELECTRONIC SUPPLEMENTARY INFORMATION

# Click-conjugated photon-upconversion nanoparticles in an immunoassay for honeybee pathogen *Melissococcus plutonius*

Veronika Poláchová,[a,b] Matěj Pastucha,[a,b] Zuzana Mikušová,[a,b] Matthias J. Mickert,[c] Antonín Hlaváček,[d] Hans H. Gorris,[c] Petr Skládal,[a,b] Zdeněk Farka *,[a]

[a] CEITEC MU, Masaryk University, Kamenice 5, 625 00 Brno, Czech Republic

[b] Department of Biochemistry, Masaryk University, Kamenice 5, 625 00 Brno, Czech Republic

[c] Institute of Analytical Chemistry, Chemo- and Biosensors, University of Regensburg, 93053 Regensburg, Germany

[d] Institute of Analytical Chemistry of the Czech Academy of Sciences, Veveří 97, 602 00 Brno, Czech Republic

* E-mail: farka@mail.muni.cz; Telephone: +420 54949 7674

## Table of contents

**1 Material and methods** **S-2**

1.1 Chemicals and reagents S-2

1.2 Preparation of microorganism samples S-3

1.3 Preparation of antibody conjugates S-4

1.4 Development of enzyme-linked immunoassay S-5

1.5 Preparation of nanoparticles S-6

1.6 Characterization of UCNP conjugates S-8

1.7 Data analysis S-10

**2 Results and discussion** **S-11**

2.1 Antibody development, testing and enzyme-linked immunosorbent assay S-11

Figure S1: Optical microscopy images of antigen preparation S-12

Figure S2: Blocking optimization and Ab-HRP conjugate testing S-13

Figure S3: Optimization of Ab-HRP concentration and Ab-biotin testing S-14

Figure S4: Analysis of real samples using ELISA S-14

2.2 Characterization of UCNPs and their conjugates S-15
Table S1: Proteins identified in UCNP-BSA sample using LC-MS/MS S-15
Table S2: Proteins identified in UCNP-BSA-SA sample using LC-MS/MS S-17
Figure S5: Zeta potentials of UCNP conjugates S-19
Figure S6: Single-particle microscopy of UCNP-BSA-SA conjugate S-19
Figure S7: Non-specific binding of UCNP conjugates on blocked plate S-20
Figure S8: Non-specific binding of UCNP conjugates on unblocked plate S-21
Figure S9: Agarose gel electrophoresis of UCNP-streptavidin S-21
2.3 Upconversion-linked immunosorbent assay S-22
Figure S10: Optimization of Ab-biotin and UCNP-BSA-SA concentration S-22
Figure S11: Comparison of ULISA and ELISA S-22
Table S3: Overview of approaches for detection of *M. plutonius* S-23
Table S4: Overview of UCNP-based assays for bacteria detection S-24
**References** **S-25**

# 1 Material and methods

## 1.1 Chemicals and reagents

Ethanolamine hydrochloride, sodium periodate, horseradish peroxidase (HRP), sodium cyanoborohydride, glycerol, biotinamidohexanoic acid *N*-hydroxysuccinimide ester (NHS-LC-biotin), sodium azide, polyoxyethylene (5) nonylphenyl ether (Igepal CO-520), ammonium fluoride (ACS reagent, ≥98.0%), tetraethyl orthosilicate (TEOS, ≥99.0%), yttrium(III) chloride hexahydrate (99.99%), ytterbium(III) chloride hexahydrate (99.99%), erbium(III) chloride hexahydrate (99.99%), oleic acid (technical grade, 90%), and 1-octadecene (technical grade, 90%) were purchased from Sigma-Aldrich (Germany). Ammonia solution (25%, p.a.), acetone (p.a.), cyclohexane (p.a.), *N*,*N*-dimethylformamide (DMF, p.a.), sodium hydroxide (p.a.) and sulfuric acid (p.a.) were from Penta (Czech Republic). Carboxyethylsilanetriol (CEST) sodium salt (25%) in water was from abcr (Germany).

## 1.2 Preparation of microorganism samples

### 1.2.1 Cultivation of microorganisms

*M. plutonius* was cultivated in a modified *Melissococcus pluton* medium (modified ATCC Medium 1430; 7.5 g peptone, 2 g tryptone, 10 g glucose, 2.5 g yeast extract, 2 g starch, 50 mL of 1 M $KH_2PO_4/K_2HPO_4$ pH 6.7, and 950 mL of water; pH 7.2 adjusted with 5 M KOH; after autoclaving at 121 °C for 15 min and cooling down, 2.5 mL of filter-sterilized 10% solution of L-cysteine hydrochloride was added; all components were obtained from Sigma-Aldrich, Germany). The 200 µL of stock *M. plutonius* suspension was inoculated into 200 mL of freshly prepared medium and the cultivation was carried out for 3 days at 34 °C anaerobically in a closed Duran bottle without shaking.

For the cultivation of *P. alvei*, *P. larvae* and *B. laterosporus*, 200 µL of stock bacterial suspension was inoculated into 200 mL of sterile medium (8 $g \cdot L^{-1}$ of Nutrient broth No. 4, Sigma-Aldrich, Germany) in Duran bottle. The incubation was done aerobically with mild shaking for 2 days at 30 °C in case of *P. alvei* and *P. larvae* and overnight at 30 °C in case of *B. laterosoporus*.

The obtained bacterial suspensions were harvested into PBS (two times centrifuged at 7,000 *g* for 10 min and resuspended in PBS). The bacteria concentrations were determined from optical density at 600 nm using McFarland standards. The aliquots of bacteria in PBS in concentration of $1 \times 10^{10}$ $CFU \cdot mL^{-1}$ were stored at −30 °C for further use.

### 1.2.2 Preparation of antigen

Cell wall fraction of *M. plutonius* was used as the immunization antigen for the development of rabbit polyclonal antibody. For the antigen preparation, 20 mL of *M. plutonius* suspension ($1 \times 10^{10}$ $CFU \cdot mL^{-1}$) in PBS was homogenized using sonicator Q700 (Qsonica, USA) with 1.6 mm Microtip probe. The program based on 60% amplitude, 4 s on time, 2 s off time, and 80 min total on time was used, resulting in total transferred energy of 120 kJ; the sample was cooled in an ice bath during the whole process. The suspension was centrifuged two times at 300 *g* for 15 min with pellet discarded between runs in order to remove the remaining whole bacteria and large cell fragments. Next, 1 mL aliquots of the obtained supernatant were centrifuged at 20,000 *g* for 2 h. The resulting pellet of antigen was resuspended in PBS (200 µL per aliquot) and frozen at −30 °C.

### 1.2.3 Processing of real samples

Samples of healthy bees, larvae and bottom hive debris were collected from apiary in the South Moravian Region, Czech Republic, in June 2018. Adult worker bees were collected from brood nests. Larvae (older specimens, around 4–5 days old) were scraped by a small spatula from uncapped brood cells. Bottom hive debris was collected from the hive bottom board. All samples were closed in plastic bags and immediately placed on dry ice. After transfer to the laboratory, they were stored at −30 °C until further use.

Before the analysis, adult bees were ground using a mortar and a pestle under liquid nitrogen[1] and transferred to a test tube. PBS-T extraction buffer (50 mM $NaH_2PO_4/Na_2HPO_4$, pH 7.4, 150 mM NaCl, 0.01% Tween 20) was added (0.5 mL per bee) and the suspension was shaken vigorously for 10 min. The sample was then centrifuged at 500 *g* for 2 min, the pellet was discarded and the supernatant was diluted 4 times or 10 times by assay buffer to reduce the matrix effect.[2] The samples for ULISA analysis were prepared by spiking *M. plutonius* in concentration from $10^2$ to $10^9$ CFU·mL$^{-1}$ to the prepared matrix.

Samples of larvae were prepared and spiked in the same manner, however due to the soft nature of the sample, mortar and pestle was replaced by a Potter-Elvehjem homogenizer (at room temperature), 0.5 mL of PBS-T per larva was added before the homogenization. Bottom hive debris was shaken directly in PBS-T (1 mL per 0.5 g) with no preceding homogenization, subsequent steps followed the same procedure.

In order to validate the precision of the ULISA assay, the concentrations of *M. plutonius* in spiked samples determined by ULISA were compared with the known amounts of bacteria spiked to the samples, as determined by turbidimetry (measurement of $OD_{600}$ with calibration using McFarland standards). First, the ULISA calibration curve was constructed, followed by spiking real samples with known amounts of bacteria and their analysis by ULISA. The concentrations corresponding to the measured signals were read out from the calibration curve and plotted against the known spiked concentrations.

## 1.3 Preparation of antibody conjugates

### 1.3.1 Conjugation of antibody with horseradish peroxidase

The conjugation of anti-*Melissococcus* antibody with HRP followed a procedure published in our previous work,[3] based on protocols by Hermanson[4] and Catty.[5] Sugar moieties on the HRP

(3.5 mg·mL$^{-1}$ in deionized water) were partially oxidized using 8 mM sodium periodate (10 min, 22 °C, mild shaking, in the dark). The reaction was quenched by the addition of glycerol (final concentration of 50 mM) and the oxidized HRP was purified and transferred to 5 mM sodium acetate buffer, pH 4.4 using the Microcon centrifugal unit YM-10 (10 kDa MWCO; Merck Millipore, USA).

For the conjugation, 5 times molar excess of the oxidized HRP was added to the antibody. The final concentrations of antibody and HRP in the reaction mixture (100 mM $Na_2CO_3$/$NaHCO_3$, pH 9.5) were 1 mg·mL$^{-1}$ and 1.47 mg·mL$^{-1}$, respectively. After 2 h of mild shaking at 22 °C in the dark, 10 μL of sodium cyanoborohydride (5 M solution in 1 M NaOH) per 1 mL of the mixture was added to specifically reduce the formed Schiff base (4 °C, overnight). The unreacted aldehyde groups on the oxidized HRP were quenched by the addition of 50 μL of 1 M ethanolamine (pH 9) per 1 mL of solution (30 min, 22 °C, mild shaking). The conjugate was purified and transferred to PBS using the Amicon Ultra 0.5 mL centrifugal filters 100K (100 kDa MWCO; Merck Millipore, USA), and stored at 4 °C for further use. The final concentration of Ab-HRP conjugate was equivalent to 4.6 mg·mL$^{-1}$ of the antibody.

### 1.3.2 Conjugation of antibody with biotin

Conjugation of the anti-*Melissococcus* antibody with biotin was done according to the protocol by Hermanson.[4] NHS-LC-biotin dissolved in anhydrous DMF (40 mg·mL$^{-1}$) was added in 15 times molar excess to the anti-*Melissococcus* antibody in PBS (4.6 mg·mL$^{-1}$) as two aliquots 10 min apart. The reaction was carried out for 30 min at room temperature with mild shaking, followed by the incubation at 4 °C overnight. The Ab-biotin conjugate was purified to PBS using the Amicon Ultra 0.5 mL centrifugal filters 100K (100 kDa MWCO) and stored at 4 °C in the concentration of 4.6 mg·mL$^{-1}$.

The conjugation of BSA with biotin for non-specific binding studies was done using the same procedure with purification on Amicon Ultra 0.5 mL centrifugal filters 10K (10 kDa MWCO). The BSA-biotin was stored in the concentration of 5 mg·mL$^{-1}$.

## 1.4 Development of enzyme-linked immunoassay

Indirect ELISA was employed to test the applicability of prepared anti-*Melissococcus* antibody for specific detection of *M. plutonius*. A transparent 96-well microtiter plate with high binding capacity (Microlon, Greiner Bio-One, Austria) was coated with standard dilutions of bacteria

(*M. plutonius* as a specific target and *P. alvei*, *P. larvae*, *B. laterosporus* as negative controls) in PBS (100 µL per well) at 4 °C overnight. All subsequent steps were carried out at room temperature. After each incubation step, the plate was washed manually four times with 250 µL of washing buffer. The remaining free binding sites of each well were blocked with 200 µL of 5% powdered milk in PBS for 1 h. Thereafter, the plate was incubated with 500× diluted rabbit polyclonal anti-*Melissococcus* antibody in assay buffer for 1 h (100 µL per well). Afterwards, 100 µL of 10 000× diluted HRP-conjugated anti-rabbit antibody ($Ab_2$-HRP; 111-035-008, Jackson ImmunoResearch, USA) in assay buffer was loaded to the wells for 1 h. The enzymatic reaction was started by the addition of 100 µL of TMB substrate solution to each well. The absorbance was read out with Synergy 2 microplate reader (BioTek, USA) at 652 nm in kinetic mode, as well as at 450 nm after quenching the reaction with 1 M $H_2SO_4$ (100 µL per well).

A sandwich ELISA was optimized as a conventional method for the detection of *M. plutonius* to provide a comparison with immunoassay based on UCNP-BSA-SA conjugates. A transparent 96-well high-binding microtiter plate (Microlon) was coated with 200× diluted anti-*Melissococcus* antibody in PBS (100 µL per well) at 4 °C overnight. All subsequent steps were carried out at room temperature. After each step, the plate was washed four times with 250 µL of washing buffer. The plate was blocked with 200 µL of 5% powdered milk in PBS for 1 h. Afterwards, the standard dilutions of bacteria in assay buffer (100 µL per well) were added and incubated for 2 h. The microtiter plate was incubated for 1 h with 100 µL of 500× diluted HRP-conjugated anti-*Melissococcus* antibody (Ab-HRP) in assay buffer. TMB substrate solution (100 µL) was added to each well and the increase in the absorbance was followed at 652 nm. Finally, the reaction was stopped by the addition of 1 M $H_2SO_4$ (100 µL per well) and the absorbance was measured at 450 nm.

## 1.5 Preparation of nanoparticles

### 1.5.1 Synthesis of UCNPs

$YCl_3 \times 6\ H_2O$ (1303 mg, 4.296 mmol), $YbCl_3 \times 6\ H_2O$ (186 mg, 0.480 mmol) and $ErCl_3 \times 6\ H_2O$ (9.2 mg, 0.024 mmol) were dissolved in 20 mL of methanol and added into a 100 mL three necked round bottom flask containing 12 mL of oleic acid and 30 mL of 1-octadecene. The solution was heated to 160 °C for 30 min under an argon atmosphere and then cooled to 50 °C. Then, the protective atmosphere was disconnected and the solution of $NH_4F$ (710 mg, 19.2 mmol) and NaOH

(480 mg, 12 mmol) in 20 mL of methanol was added to the intensively stirred solution. The argon atmosphere was reconnected and the solution was stirred for 30 min. The temperature was carefully increased up to 150 °C avoiding extensive boiling to ensure the evaporation of methanol. Thereafter, the solution was rapidly heated using a rate of 10 °C per minute. At 300 °C, the heating was carefully regulated to 305 °C within one or two minutes. The flask was kept under argon flow at 305 °C for 150 min. The fluctuation of temperature was ±3 °C during this time. Finally, the flask was placed on another stirrer and rapidly cooled to room temperature under air flux. The resulting nanoparticles were precipitated by adding 42 mL of isopropanol and collected by centrifugation (3,000 *g*, 10 min). The pellet was washed with 40 mL of methanol, centrifuged (3,000 *g*, 10 min) and redispersed in 40 mL of cyclohexane. Upon adding 200 mL of methanol, the UCNPs precipitated rapidly without the need for centrifugation.[6] The wax-like precipitate was finally redispersed in 40 mL of cyclohexane to a concentration of 13.1 $mg \cdot mL^{-1}$ in a yield of 524 mg.

### 1.5.2 Silanization of UCNPs

UCNPs (418 mg) were diluted in cyclohexane to a volume of 36.8 mL and 4600 mg of Igepal CO-520 was added to the dispersion with 251 µL of TEOS and stirred with high intensity for 10 min. The microemulsion formed after adding 558 µL of 12% (w/v) aqueous ammonium hydroxide and it was slowly stirred overnight. Another 126 µL of TEOS was added and the microemulsion was slowly stirred for 4 hours. CEST (25% in water, 251 µL) was added and the cloudy emulsion was sonicated for 15 min and further stirred for 60 min. Carboxylated UCNPs were extracted by adding 5 mL of DMF and washed 4 times with 2 mL of acetone and 5 times with 6 mL of water. For estimating UCNP mass concentrations, 200 µL of water dispersion of UCNPs was filled into a glass vial. The vial was placed first on a heater to evaporate water and then for 3 hours in an oven at 450 °C. The carboxylated UCNPs were stored as an aqueous dispersion at a concentration of 37 $mg \cdot mL^{-1}$.[7, 8]

### 1.5.3 Conjugation of silanized UCNPs with streptavidin via carboxyl groups

For the conjugation, 10 mg of carboxylated silica-coated UCNPs were dispersed in 2.0 mL of 100 mM 2-(*N*-morpholino)ethanesulfonic acid (MES) and 30 mM $Na_2CO_3$, pH 6.0, and activated by 4 mg of EDC (21 µmol) and 2 mg of NHS (9 µmol) for 15 min at room temperature. The activated UCNPs were rapidly centrifuged (1,700 *g*, 1 min), dispersed in 2.0 mL of 100 mM MES, 30 mM $Na_2CO_3$, pH 6.0, which contained 5 mg of dissolved streptavidin. After 60 min at room temperature, the UCNP-streptavidin conjugate was centrifuged (1,700 *g*, 20 min) three times and

dispersed in Tris-borate buffer (TB; 50 mM tris(hydroxymethyl)aminomethane, 50 mM $H_3BO_3$, pH 8.6) to a final UCNP concentration of 20.0 mg·mL$^{-1}$. The conjugate was stored at 4 °C in TB buffer supplemented with 0.05% $NaN_3$.

## 1.6 Characterization of UCNP conjugates

### 1.6.1 Transmission electron microscopy

A 400-mesh copper EM grid coated with a continuous carbon layer was first modified by adsorption of cationized bovine serum albumin (6 µL, 1 mg·mL$^{-1}$ in water) and incubated at room temperature for 5 min. Silica-coated UCNPs were diluted in 10 mM MES (pH 6.1 set by NaOH). After 10 washing steps with 10 µL of water, a 6 µL droplet of the UCNP-silica dispersion was deposited on the grid surface and incubated for 5 min at room temperature. Finally, the grid was washed 10 times with 10 µL of water.[9] Dried grids were imaged by transmission electron microscope Tecnai F20 (FEI, Czech Republic). The dimensions of individual particles were analyzed using ImageJ imaging software (National Institutes of Health, USA).[10]

### 1.6.2 Emission spectra measurement

For the measurement of emission spectra, 0.5 µL droplet of UCNP dispersion in water (1 mg·mL$^{-1}$) was placed between two glass slides with 100 µm spacer. The excitation was performed using continuous 980 nm laser (5 W; Laserland, China), the spectrum was collected as an average of 100 repeated measurements with 100 ms integration time using CCD array spectroscope QE65 Pro (Ocean Optics, USA).

### 1.6.3 Agarose gel electrophoresis

Electrophoretic buffer (45 mM Tris, 45 mM $H_3BO_3$, pH 8.6) was used for preparation of agarose gel and for the gel electrophoresis.[7] Samples were diluted with electrophoretic buffer to a final UCNP concentration of 1 mg·mL$^{-1}$. The volume of 20 µL of each sample was supplemented with 4.5 µL of 50% (w/w) glycerol and loaded on a 0.3% agarose gel. The electrophoresis was performed at 7.5 V·cm$^{-1}$ for 50 min at room temperature. The gel was subsequently scanned for fluorescence of CF (488/530 nm) and Rh (532/605 nm) on Molecular Imager PharosFX (Bio-Rad, USA) and for upconversion luminescence in the range of 646–672 nm using a laboratory-build scanner equipped with continuous 980 nm laser (5 W) and CCD spectroscope QE65 Pro (Ocean Optics, USA) as a detector.

### 1.6.4 LC-MS/MS analysis

The presence of BSA and streptavidin conjugated on UCNPs was further confirmed by LC-MS/MS analysis. The samples of UCNP-BSA and UCNP-BSA-SA (100 µL, 5 $mg \cdot mL^{-1}$) were washed twice by 200 µL of 50 mM ammonium bicarbonate buffer (AB), followed by resuspending in 15 µL of AB. Cysteine residues of proteins were reduced and alkylated by iodoacetamide, and the proteins were digested by trypsin (1 µg, 2 h, 37 °C). The UCNPs were removed by centrifugation (14,000 *g*, 10 min) and the generated peptides were extracted using acetonitrile (addition of acetonitrile was followed by vortexing of the sample and evaporation of acetonitrile by rotary evaporator to a final volume of 15 µL).

The LC-MS/MS analysis was performed using RSLCnano and Orbitrap Elite (Thermo Fisher Scientific, USA). The 65 min LC gradient was used for LC-MS analyses, MS spectra were recorded in Orbitrap analyzer (resolution of 60 000 at 400 *m*/*z*), and MS/MS (after HCD fragmentation) was recorded in Orbitrap analyzer (resolution 15 000 at 400 *m*/*z*). The MS/MS data were processed using Proteome Discoverer software (version 1.4; Thermo Fisher Scientific, USA). The search engine Mascot (version 2.6; Matrix Science, USA) was used to search cRAP contaminant database (version 181122; The Global Proteome Machine Organization, http://www.thegpm.org/crap/), which contains 112 protein sequences, including target sequences of BSA (P02769-cRAP-B6E) and streptavidin (P22629-cRAP). Peptide confidence was evaluated based on Mascot expectation value, only peptides above significance threshold were considered for final data evaluation.

### 1.6.5 Dynamic light scattering

For estimating the hydrodynamic diameters, DLS in dispersions containing 10 $\mu g \cdot mL^{-1}$ of UCNPs in 50 mM $H_3BO_3$ and 50 mM Tris was measured. The same dispersions were used also for estimating the zeta-potentials. Both measurements were made on a Zetasizer Nano ZS (Malvern, UK).

### 1.6.6 Single-particle upconversion microscopy

For the visualization of individual UCNPs, inverted optical microscope Eclipse Ti-E (Nikon, Japan) equipped with a 980 nm continuous wave laser diode (4 W, WSLS-980-004-H-T, Wavespectrum, China) coupled via a multimode optical fiber (105 µm fiber core, NA 0.22, Wavespectrum), a 100× objective with a NA of 1.49 (CFI HP Apochromat TIRF, Nikon), and a 5.5-megapixel vacuum cooled sCMOS camera (Neo, Andor Technology, UK) was used. The

optical filter cube consisted of a long-pass excitation filter ($\lambda_{cut\text{-}on}$ = 875 nm, Schott, Germany), a dichroic mirror for multiphoton applications ($\lambda_{cut\text{-}on}$ = 830 nm, AHF Analysentechnik, Germany), and a band-pass filter transparent for green emission of $Er^{3+}$-doped UCNPs ($\lambda$ = 535±70 nm, Chroma, USA).[9]

To evaluate the intensity distribution of the conjugates, UCNP-BSA-SA was adsorbed on surface of a high-binding 96-well polystyrene microtiter plate with 190 μm thick bottom foil (μCLEAR, Greiner Bio-One, Austria), which is suitable for the working distance of the high NA immersion oil objective. The images were taken with 1 s exposure time and the mean intensities of the individual UCNPs were determined in the microscope software (NIS elements, Nikon) by placing regions of interest (ROIs) of identical sizes over the luminescent spots. Mean intensities of 400 randomly selected UCNPs were measured and background corrected, frequency count was performed and the data were arranged in a histogram.

### 1.6.7 Non-specific binding studies

Microtiter plate-based assay was employed to study the effect of BSA modification on the level of non-specific binding. In the first experimental design, the plate was coated overnight with 100 μL of samples diluted in PBS, blocked with 200 μL of 5% powdered milk in PBS for 1 h, and incubated with sample of UCNPs (10 $\mu g \cdot mL^{-1}$ in assay buffer, 100 μL per well) for 1 h. Alternatively, the plate was coated overnight with proteins in PBS, followed by binding of UCNPs in PBS (10 $\mu g \cdot mL^{-1}$, 100 μL per well). After each step, the plate was washed four times with 250 μL of washing buffer. The luminescence intensities were read out from dry plate using the same procedure as in ULISA assay.

## 1.7 Data analysis

For each concentration, the average and standard deviation were calculated from three replicate wells. A four-parameter logistic model was used for the regression analysis of the calibration curves:

$$y = \frac{y_{\mathrm{MAX}} - y_{\mathrm{BG}}}{1 + \left(\frac{c}{EC_{50}}\right)^{s}} + y_{\mathrm{BG}}$$

where $c$ is the concentration of *M. plutonius*, and $y$ is the measured signal (upconversion luminescence or absorbance at 450 nm). The parameter $y_{\mathrm{MAX}}$ marks the highest point of the sigmoidal curve while $y_{\mathrm{BG}}$ is the lowest point corresponding to the background signal. The point

where the difference between $y_{MAX}$ and $y_{BG}$ is reduced by 50% is the half maximal effective concentration or $EC_{50}$, the slope at the inflection point is indicated as $s$. The limit of detection (LOD) was calculated from the regression curve as the concentration corresponding to the $y_{LOD}$ value:

$$y_{LOD} = y_{BG} + 3\, s_0$$

where $s_0$ is the standard deviation of blank measurement (no analyte present in the sample).

# 2 Results and discussion

## 2.1 Antibody development, testing and enzyme-linked immunosorbent assay

The assay for European foulbrood diagnosis was intended to be carried out by specialized laboratories in bee material (bees, larvae, bottom hive debris) taken by beekeepers in the examined apiaries. To make the assay effective and suitable for practical use, only a few uncomplicated sample processing steps should be required in the laboratory. This would leave most of the bacterial cells either intact or with minor damage, but without proper disruption or homogenization of cells. Therefore, the antibodies should be specific to "whole cells" of *M. plutonius*, or – at the molecular level – to epitopes on the outer side of the bacterial peptidoglycan layer. As looking for a suitable specific molecular marker on the bacteria surface would be a tedious task without any guarantee of success, immunizing the rabbit with whole bacterial antigen or a proper fraction of bacterial fragments is a quicker, cheaper and thus a more practical way to generate functional specific antibodies. The use of whole bacteria could look like a method of choice, as the bacteria administered to the antibody producing animal (rabbit) would be in the practically same form as in the sample for analysis. However, due to the decomposition of bacterial cells by rabbit immune system, antibodies to other than surface epitopes would be probably also produced, lowering the overall specificity of the polyclonal antibody towards the whole bacteria. Therefore, cell wall fraction was used as the antigen for polyclonal antibody preparation. Optical microscopy images comparing native *M. plutonius*, sonicated cells, and purified antigen are shown in **Figure S1**.

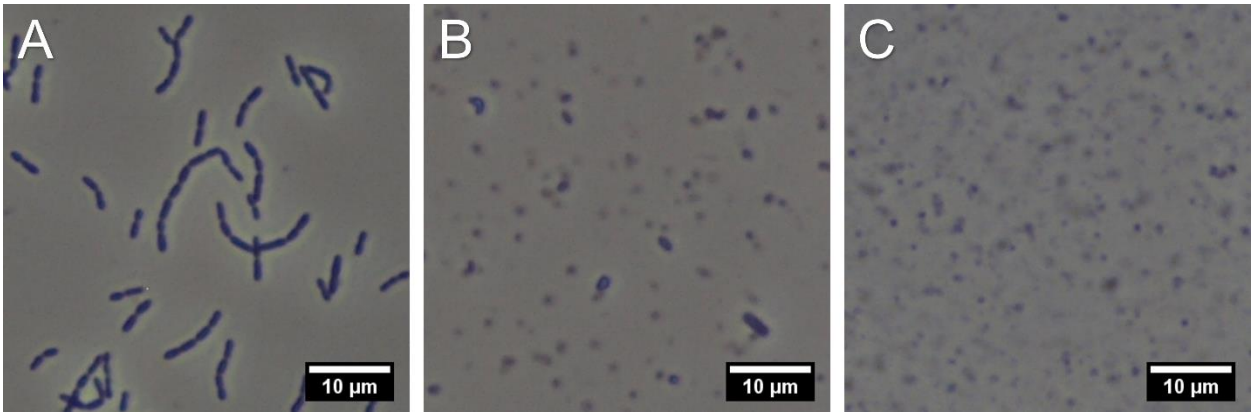


**Figure S1:** Optical microscopy images of **(A)** native *M. plutonius*, **(B)** bacterial cells homogenized by sonication, and **(C)** purified cell wall fraction. The images were acquired using microscope Olympus BX41 equipped with 40× objective, phase contrast condenser U-PCD2, and camera Olympus E-510 (Olympus, Japan).

For the optimization of blocking conditions (**Figure S2A**), three blocking buffers were compared, based on 5% powdered milk in PBS, 1% BSA in PBS, and 1% BSA in assay buffer. Nevertheless, the similar results obtained for all these conditions suggest that the choice of blocking solution does not significantly affect the assay properties. For further experiments, blocking by powdered milk was selected due to slightly smaller standard deviations and lower signals for the negative control compared to blocking by BSA.

The indirect ELISA for *M. plutonius* detection, intended mainly for testing of the antibody, was based on two antibodies; primary rabbit anti-*Melissococcus* antibody and secondary anti-rabbit antibody conjugated with HRP ($Ab_2$-HRP). However, such application of secondary antibody was not suitable for sandwich arrangement due to the presence of rabbit anti-*Melissococcus* antibody coated on the microtiter plate. Therefore, the anti-*Melissococcus* antibody was conjugated directly with HRP (Ab-HRP). To test the functionality of the prepared conjugate, direct assay format with bacteria coated on the plate was employed prior to the complete sandwich and the assay utilizing the Ab-HRP was compared with the use of native anti-*Melissococcus* antibody in combination with $Ab_2$-HRP (**Figure S2B**). Both assays provided comparable LODs, with even slightly higher signals in case of Ab-HRP, which confirms that the conjugation was successful and that the conjugate quality does not deteriorate the assay properties.

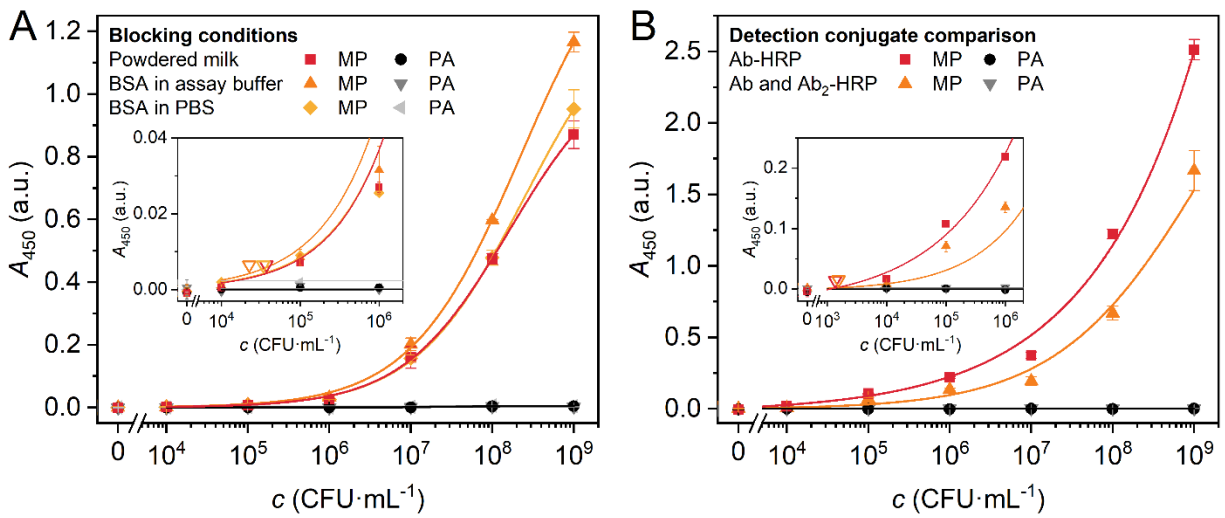


**Figure S2: (A)** Optimization of blocking conditions of indirect ELISA for detection of *M. plutonius* (MP), with *P. alvei* (PA) as a negative control. **(B)** Comparison of direct ELISA based on Ab-HRP with indirect ELISA based on Ab and $Ab_2$-HRP. Open triangles represent the LOD values.

Conjugate of anti-*Melissococcus* antibody with biotin (Ab-biotin) was prepared in order to achieve highly sensitive sandwich immunoassay based on UCNP-BSA-SA label. The functionality of the Ab-biotin was first tested in a sandwich assay using conjugate of streptavidin with horseradish peroxidase (SA-HRP; ab7403, Abcam, UK) as a detection label (**Figure S3B**). The increasing concentrations of SA-HRP resulted in increasing measured absorbance, however, without significant effect on achieved LOD value. Overall, all tested assay arrangements (indirect with secondary $Ab_2$-HRP, direct sandwich based on Ab-HRP, and indirect sandwich based on Ab-biotin and SA-HRP) provided similar sensitivity, suggesting that the assay is limited mainly by the affinity of the antibody and sensitivity of absorbance readout for the HRP-based label.

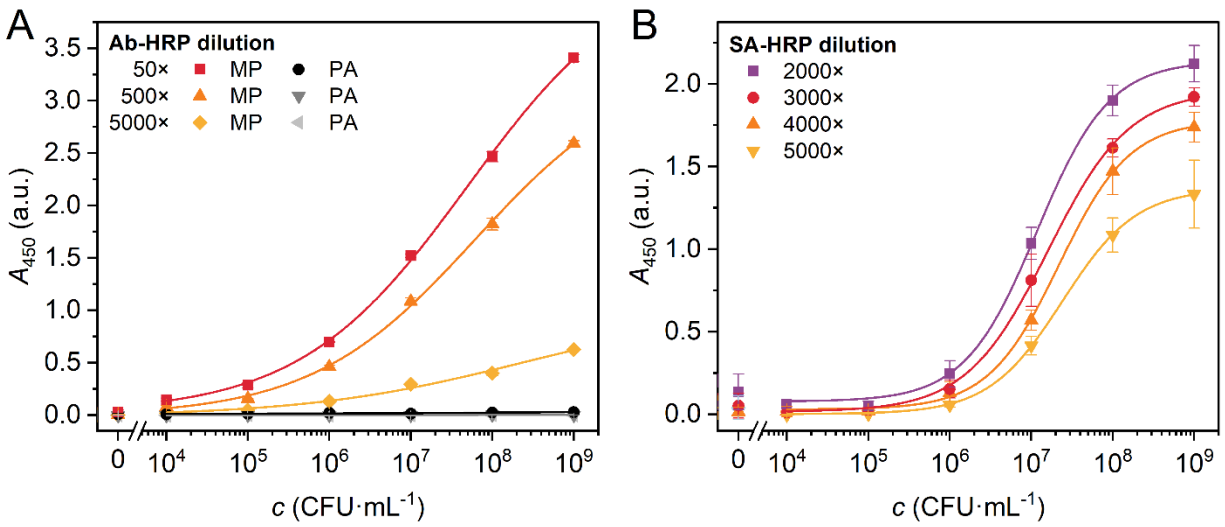


**Figure S3: (A)** Optimization of concentration of anti-*Melissococcus* antibody conjugated with HRP (Ab-HRP) in direct sandwich ELISA. **(B)** Testing of anti-*Melissococcus* antibody conjugated with biotin (Ab-biotin) in indirect sandwich ELISA with streptavidin-HRP (SA-HRP) as a label.

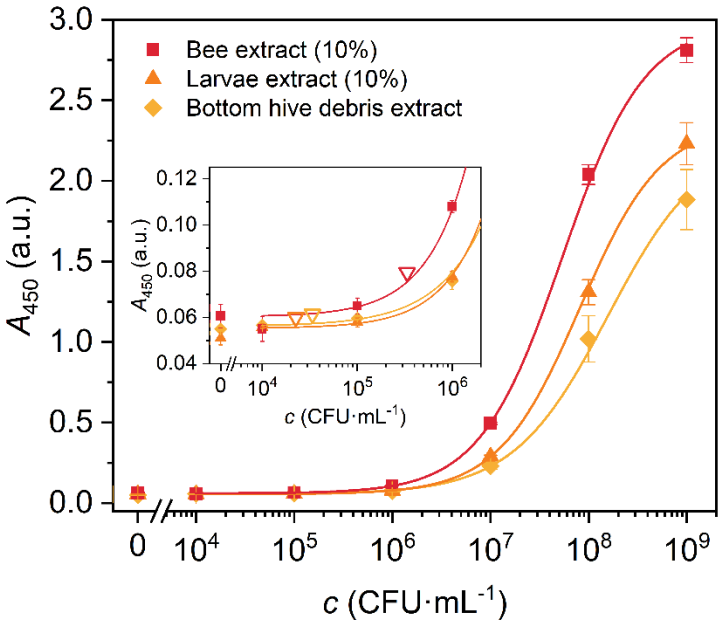


**Figure S4:** Calibration curves of sandwich ELISA for detection of *M. plutonius* spiked in real samples of bees, larvae and bottom hive debris. Open triangles represent the LOD values.

## 2.2 Characterization of UCNPs and their conjugates

**Table S1:** Proteins identified in the UCNP-BSA sample using LC-MS/MS.

| **Protein group[a]** | **Accession ID** | **Description** | **Area[b] (a.u.)** | **Coverage[c]** | **Peptides[d]** | **Unique peptides[e]** |
|---|---|---|---|---|---|---|
| **1** | **P02769-cRAP-B6E** | **Serum albumin (cRAP-B6E) OS=*Bos taurus* GN=ALB PE=1 SV=4 - [ALBU_BOVIN]** | **$1.38\times10^{10}$** | **90%** | **101** | **93** |
| 2 | P00761-cRAP | Trypsin (cRAP) OS=*Sus scrofa* PE=1 SV=1 - [TRYP_PIG] | $1.30\times10^{10}$ | 77% | 12 | 12 |
| 3 | P02768-cRAP | Serum albumin (cRAP) OS=*Homo sapiens* GN=ALB PE=1 SV=2 - [ALBU_HUMAN] | $1.18\times10^{10}$ | 14% | 10 | 2 |
| 4 | P04264-cRAP | Keratin, type II cytoskeletal 1 (cRAP) OS=*Homo sapiens* GN=KRT1 PE=1 SV=6 - [K2C1_HUMAN] | $2.55\times10^{8}$ | 62% | 44 | 39 |
| 5 | P35908-cRAP | Keratin, type II cytoskeletal 2 epidermal (cRAP) OS=*Homo sapiens* GN=KRT2 PE=1 SV=2 - [K22E_HUMAN] | $1.50\times10^{8}$ | 50% | 30 | 18 |
| 6 | P35527-cRAP | Keratin, type I cytoskeletal 9 (cRAP) OS=*Homo sapiens* GN=KRT9 PE=1 SV=3 - [K1C9_HUMAN] | $1.47\times10^{8}$ | 66% | 30 | 29 |
| 7 | iRT-fusion-cRAP | iRT Kit Fusion - real (cRAP) - [iRT_Fusion] | $1.25\times10^{8}$ | 91% | 10 | 10 |
| 8 | P13645-cRAP | Keratin, type I cytoskeletal 10 (cRAP) OS=*Homo sapiens* GN=KRT10 PE=1 SV=6 - [K1C10_HUMAN] | $1.06\times10^{8}$ | 60% | 31 | 25 |
| 9 | P02533-cRAP | Keratin, type I cytoskeletal 14 (cRAP) OS=*Homo sapiens* GN=KRT14 PE=1 SV=4 - [K1C14_HUMAN] | $1.06\times10^{8}$ | 62% | 30 | 8 |
| 10 | P08779-cRAP | Keratin, type I cytoskeletal 16 (cRAP) OS=*Homo sapiens* GN=KRT16 PE=1 SV=4 - [K1C16_HUMAN] | $1.06\times10^{8}$ | 60% | 29 | 12 |
| 11 | K7ERE3-cRAP | Keratin, type I cytoskeletal 13 (cRAP) OS=*Homo sapiens* GN=KRT13 PE=1 SV=1 - [K7ERE3_HUMAN] | $8.91\times10^{7}$ | 13% | 7 | 1 |
| 12 | H0Y8D1-cRAP | Trypsin-1 (Fragment) (cRAP) OS=*Homo sapiens* GN=PRSS1 PE=3 SV=1 - [H0Y8D1_HUMAN] | $8.36\times10^{7}$ | 7% | 1 | 1 |

| | | | | | | |
|---|---|---|---|---|---|---|
| 13 | Q04695-cRAP | Keratin, type I cytoskeletal 17 (cRAP) OS=*Homo sapiens* GN=KRT17 PE=1 SV=2 - [K1C17_HUMAN] | $7.99\times10^{7}$ | 32% | 17 | 3 |
| 14 | P13647-cRAP | Keratin, type II cytoskeletal 5 (cRAP) OS=*Homo sapiens* GN=KRT5 PE=1 SV=3 - [K2C5_HUMAN] | $7.08\times10^{7}$ | 30% | 23 | 8 |
| 15 | P02538-cRAP | Keratin, type II cytoskeletal 6A (cRAP) OS=*Homo sapiens* GN=KRT6A PE=1 SV=3 - [K2C6A_HUMAN] | $7.08\times10^{7}$ | 41% | 29 | 12 |
| 16 | Q5T749-cRAP | Keratinocyte proline-rich protein (cRAP) OS=*Homo sapiens* GN=KPRP PE=1 SV=1 - [KPRP_HUMAN] | $6.65\times10^{6}$ | 3% | 2 | 2 |
| 17 | Q5D862-cRAP | Filaggrin-2 (cRAP) OS=*Homo sapiens* GN=FLG2 PE=1 SV=1 - [FILA2_HUMAN] | $4.46\times10^{6}$ | 1% | 2 | 2 |
| 18 | P15924-2-cRAP | Isoform DPII of Desmoplakin (cRAP) OS=*Homo sapiens* GN=DSP - [DESP_HUMAN] | $4.20\times10^{6}$ | 1% | 2 | 2 |
| 19 | Q02413-cRAP | Desmoglein-1 (cRAP) OS=*Homo sapiens* GN=DSG1 PE=1 SV=2 - [DSG1_HUMAN] | $2.31\times10^{6}$ | 1% | 1 | 1 |

[a] Proteins from the target database containing the same set of peptides are reported within one protein group. Protein groups are ordered based on the area

[b] Protein group area calculated as mean abundance of three most abundant peptides identified for particular protein group

[c] Percentage of protein sequence covered by identified peptides

[d] Number of peptides assigned to protein group including peptides that are shared with other protein groups

[e] Number of peptides that are “unique” for particular protein group. Number is considered within the given protein group list, not from all proteins present in the used protein database

**Table S2:** Proteins identified in the UCNP-BSA-SA sample using LC-MS/MS.

| Protein group[a] | Accession ID | Description | Area[b] (a.u.) | Coverage[c] | Peptides[d] | Unique peptides[e] |
|---|---|---|---|---|---|---|
| **1** | **P02769-cRAP-B6E** | **Serum albumin (cRAP-B6E) OS=*Bos taurus* GN=ALB PE=1 SV=4 - [ALBU_BOVIN]** | **$1.58\times10^{10}$** | **85%** | **81** | **75** |
| 2 | P02768-cRAP | Serum albumin (cRAP) OS=*Homo sapiens* GN=ALB PE=1 SV=2 - [ALBU_HUMAN] | $1.34\times10^{10}$ | 9% | 7 | 1 |
| 3 | P00761-cRAP | Trypsin (cRAP) OS=*Sus scrofa* PE=1 SV=1 - [TRYP_PIG] | $4.78\times10^{9}$ | 25% | 5 | 5 |
| **4** | **P22629-cRAP** | **Streptavidin (cRAP) OS=*Streptomyces avidinii* PE=1 SV=1 - [SAV_STRAV]** | **$1.63\times10^{9}$** | **32%** | **3** | **3** |
| 5 | P04264-cRAP | Keratin, type II cytoskeletal 1 (cRAP) OS=*Homo sapiens* GN=KRT1 PE=1 SV=6 - [K2C1_HUMAN] | $3.60\times10^{8}$ | 59% | 35 | 31 |
| 6 | P35527-cRAP | Keratin, type I cytoskeletal 9 (cRAP) OS=*Homo sapiens* GN=KRT9 PE=1 SV=3 - [K1C9_HUMAN] | $2.53\times10^{8}$ | 64% | 30 | 29 |
| 7 | P35908-cRAP | Keratin, type II cytoskeletal 2 epidermal (cRAP) OS=*Homo sapiens* GN=KRT2 PE=1 SV=2 - [K22E_HUMAN] | $2.14\times10^{8}$ | 32% | 17 | 12 |
| 8 | P13645-cRAP | Keratin, type I cytoskeletal 10 (cRAP) OS=*Homo sapiens* GN=KRT10 PE=1 SV=6 - [K1C10_HUMAN] | $1.36\times10^{8}$ | 47% | 21 | 17 |
| 9 | iRT-fusion-cRAP | iRT Kit Fusion - real (cRAP) - [iRT_Fusion] | $1.26\times10^{8}$ | 100% | 11 | 11 |
| 10 | P02533-cRAP | Keratin, type I cytoskeletal 14 (cRAP) OS=*Homo sapiens* GN=KRT14 PE=1 SV=4 - [K1C14_HUMAN] | $1.03\times10^{8}$ | 20% | 9 | 2 |
| 11 | P08779-cRAP | Keratin, type I cytoskeletal 16 (cRAP) OS=*Homo sapiens* GN=KRT16 PE=1 SV=4 - [K1C16_HUMAN] | $1.03\times10^{8}$ | 20% | 9 | 2 |
| 12 | P02538-cRAP | Keratin, type II cytoskeletal 6A (cRAP) OS=*Homo sapiens* GN=KRT6A PE=1 SV=3 - [K2C6A_HUMAN] | $7.47\times10^{7}$ | 12% | 6 | 2 |

| | | | | | | |
|---|---|---|---|---|---|---|
| 13 | P13647-cRAP | Keratin, type II cytoskeletal 5 (cRAP) OS=*Homo sapiens* GN=KRT5 PE=1 SV=3 - [K2C5_HUMAN] | $6.97\times10^{7}$ | 11% | 6 | 3 |
| 14 | P05787-cRAP | Keratin, type II cytoskeletal 8 (cRAP) OS=*Homo sapiens* GN=KRT8 PE=1 SV=7 - [K2C8_HUMAN] | $6.53\times10^{7}$ | 7% | 4 | 1 |
| 15 | P00698-cRAP | Lysozyme C OS=*Gallus gallus* (cRAP) GN=LYZ PE=1 SV=1 - [LYSC_CHICK] | $4.29\times10^{7}$ | 42% | 5 | 5 |
| 16 | P14923-cRAP | Junction plakoglobin (cRAP) OS=*Homo sapiens* GN=JUP PE=1 SV=3 - [PLAK_HUMAN] | $5.36E\times10^{6}$ | 1% | 1 | 1 |
| 17 | P15924-2-cRAP | Isoform DPII of Desmoplakin (cRAP) OS=*Homo sapiens* GN=DSP - [DESP_HUMAN] | $1.16\times10^{6}$ | 0% | 1 | 1 |

[a] Proteins from the target database containing the same set of peptides are reported within one protein group. Protein groups are ordered based on the area

[b] Protein group area calculated as mean abundance of three most abundant peptides identified for particular protein group

[c] Percentage of protein sequence covered by identified peptides

[d] Number of peptides assigned to protein group including peptides that are shared with other protein groups

[e] Number of peptides that are “unique” for particular protein group. Number is considered within the given protein group list, not from all proteins present in the used protein database

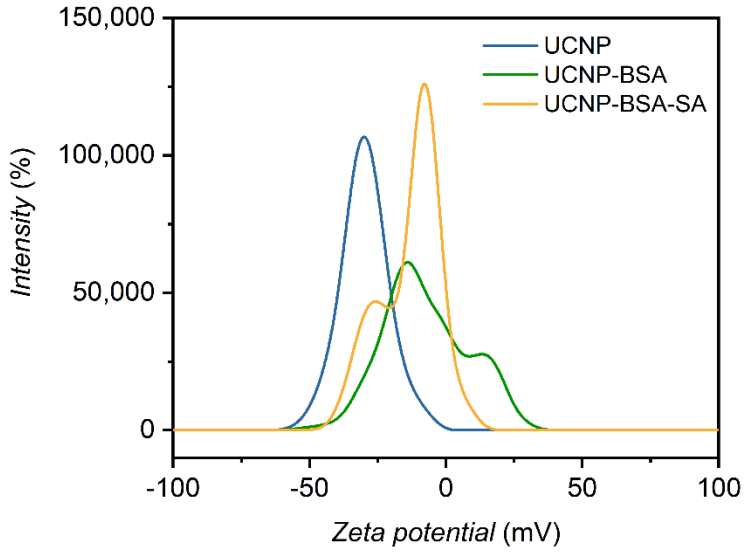


**Figure S5:** Zeta potentials of silica-coated UCNPs, UCNP-BSA, and UCNP-BSA-SA conjugates.

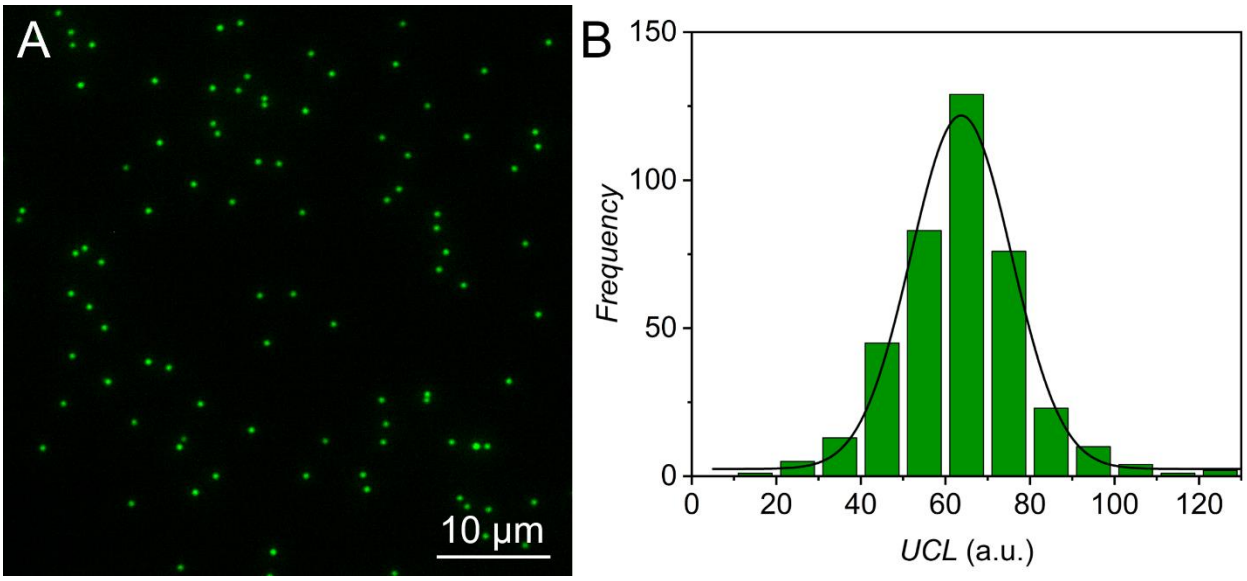


**Figure S6: (A)** Upconversion microscopy image of the UCNP-BSA-SA conjugate adsorbed on surface of a microtiter plate. **(B)** The brightness distribution of 400 luminescent spots shows coefficient of variation (calculated as SD of spot UCL / average spot UCL) of 28.9%. The black line represents a fit using Gaussian function.

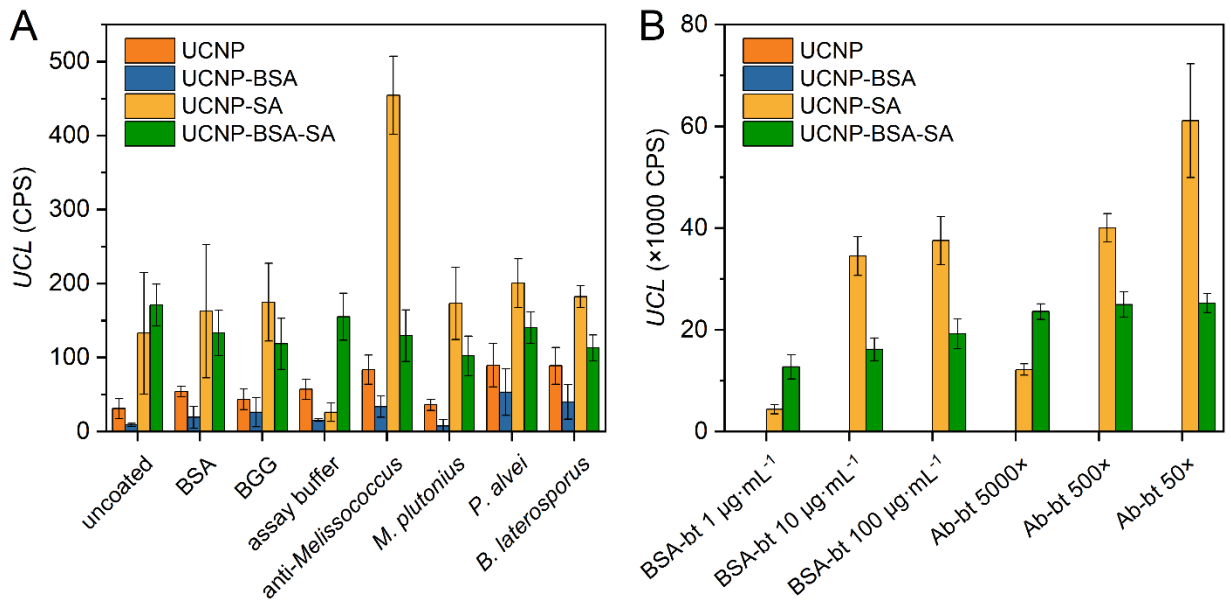


**Figure S7: (A)** The effect of surface modification of the silica-coated UCNPs on the level of non-specific binding. BSA (10 µg·mL$^{-1}$), BGG (10 µg·mL$^{-1}$), assay buffer, anti-*Melissococcus* Ab (200×), *M. plutonius* ($10^9$ CFU·mL$^{-1}$), *P. alvei* ($10^9$ CFU·mL$^{-1}$), and *B. laterosporus* ($10^9$ CFU·mL$^{-1}$) were coated on the microtiter plate, followed by blocking with 5% powdered milk in PBS and binding of UCNPs in assay buffer. **(B)** The level of binding of UCNPs with different surface modification on proteins modified by biotin (bt) coated on microtiter plate. Due to the high specific binding of streptavidin conjugates and low level of non-specific binding of unconjugated particles, the very low signals of UCNP and UCNP-BSA samples are not visible within the used scale.

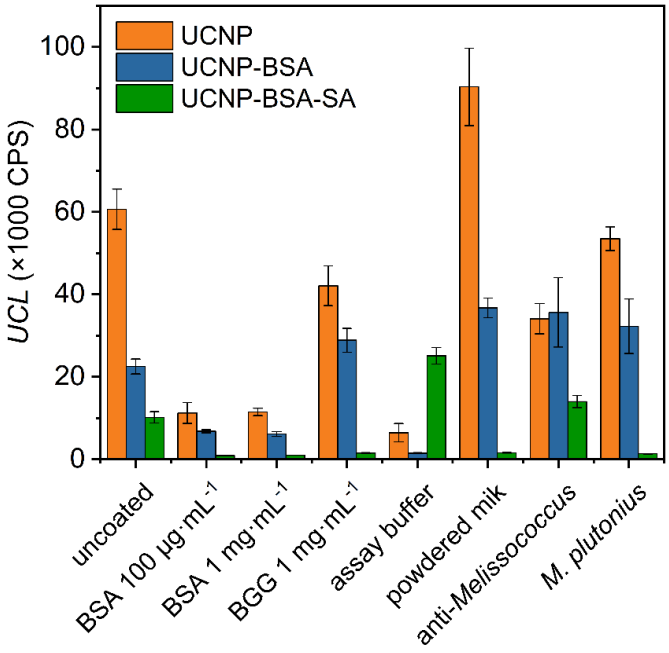


**Figure S8:** The effect of surface modification of the silica-coated UCNPs on the level of non-specific binding. BSA (100 µg·mL$^{-1}$ and 1 mg·mL$^{-1}$), BGG (1 mg·mL$^{-1}$), assay buffer, powdered milk (5%), anti-*Melissococcus* Ab (200×), and *M. plutonius* ($10^9$ CFU·mL$^{-1}$) were coated on microtiter plate, followed by binding of UCNPs in PBS (no blocking step).

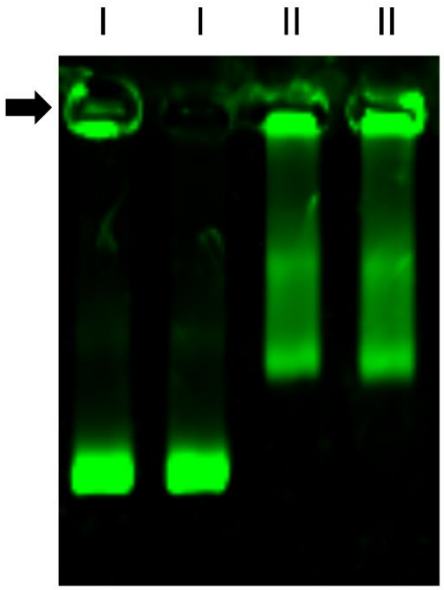


**Figure S9:** Agarose gel electrophoresis of (I) carboxylated silica-coated UCNPs and (II) UCNP-streptavidin conjugates in duplicates. The arrow indicates the starting point of electrophoresis.

## 2.3 Upconversion-linked immunosorbent assay

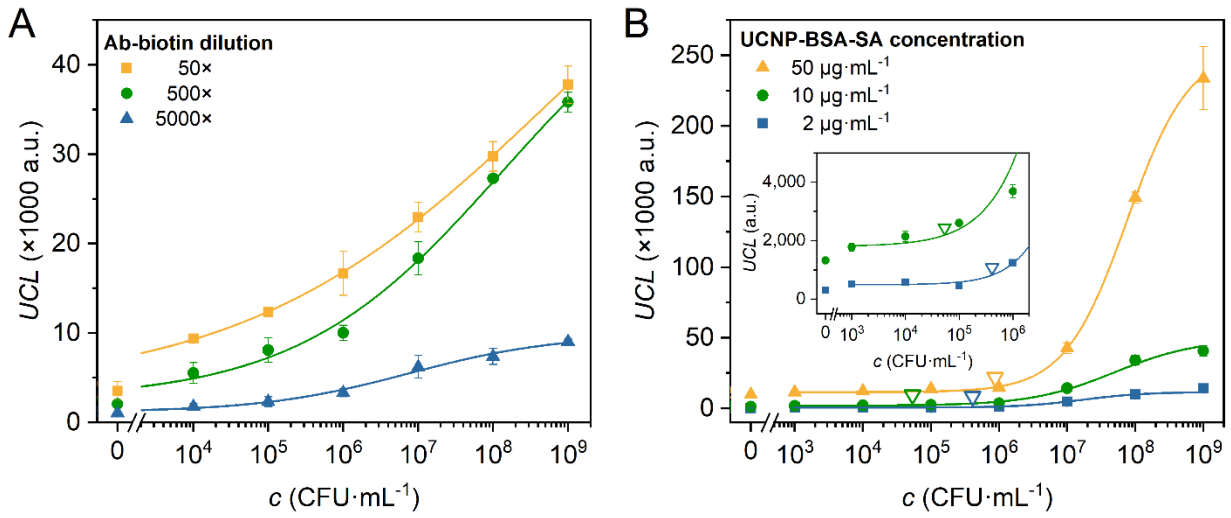


**Figure S10: (A)** Optimization of concentration of anti-*Melissococcus* antibody conjugated with biotin (Ab-biotin) in sandwich ULISA. **(B)** Optimization of UCNP-BSA-SA conjugate concentration. Open triangles represent the LOD values.

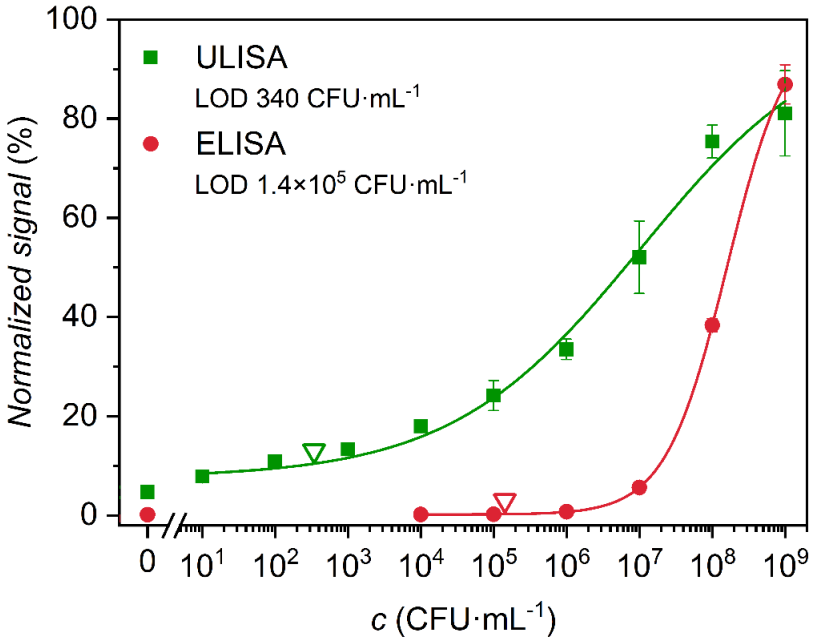


**Figure S11:** Comparison of sandwich ULISA and ELISA assays for the detection of *M. plutonius*. The normalized signals were calculated by dividing the data by $y_{MAX}$ value from the logistic fit. Open triangles represent the LOD values.

**Table S3:** Overview of approaches for laboratory detection of *M. plutonius*.

| **Method** | **LOD (CFU·mL$^{-1}$)** | **Analyzed sample** | **Note** | **Reference** |
|---|---|---|---|---|
| ULISA | 340 | Worker bees, larvae, debris | 540 CFU·mL$^{-1}$ in bee | This work |
| ELISA | $10^5$ | Bacterial culture | For Ab characterization | This work |
| ELISA | $10^5$ | Worker bees, larvae | – | 11 |
| ELISA | $10^6$ | Bacterial culture | For Ab characterization | 12 |
| LFIA | N/A | Larvae | In-field confirmation of diagnosis | 12 |
| Cultivation | ~ $5\times10^3$–$10^4$ [a] | Larvae, honey | Cultivation recovery 0.1–0.2% | 13 |
| PCR | N/A | Larvae | – | 14 |
| Hemi-nested PCR | 6 | Bacterial culture | – | 15 |
| Hemi-nested PCR | 20 fg DNA | Worker bees, larvae, honey, pollen, combs | – | 16 |
| Hemi-nested PCR | 10 fg DNA | Larvae, honey | 100 fg DNA in larvae samples ($10^3$ CFU·mL$^{-1}$) | 17 |
| Real-time PCR | 3.5 | Worker bees | – | 18 |
| Real-time PCR | N/A | Worker bees, larvae | Changes in *M. plutonius* levels after treatment | 19 |
| Duplex PCR | 50 copies of DNA | Bacterial culture | Discrimination between typical and atypical strains of *M. plutonius* | 20 |
| Triplex PCR | 1 pg DNA (456 copies of DNA) | Larvae | Simultaneous detection of *M. plutonius*, *P. larvae* and *A. mellifera* DNA | 21 |
| AuNP-based DNA assay | 50 fg DNA (25 copies of DNA) | Larvae | Requires extraction of DNA, but no PCR amplification | 22 |
| Next-generation sequencing | N/A | Worker bees | Relative numbers (microbiome analysis) | 23 |

Ab – antibody; LFIA – lateral-flow immunoassay; PCR – polymerase chain reaction; AuNP – gold nanoparticle

[a] Estimated from the reported cultivation recovery 0.1–0.2% and 100 µL plated volume.

**Table S4:** Overview of assays for bacteria detection based on UCNPs.

| **Method** | **Nanoparticle label** | **Target bacteria** | **LOD (CFU·mL$^{-1}$)** | **Working range (CFU·mL$^{-1}$)** | **Reference** |
|---|---|---|---|---|---|
| Sandwich ULISA | UCNP-BSA-SA | *Melissococcus plutonius* | 340 | 340–$10^9$ | This work |
| LFIA | UCNP-Ab | *Vibrio anguillarum* | 100 | $10^3$–$10^9$ | 24 |
| LFIA | UCNP-Ab | Multiple bacteria[a] | $10^4$ to $10^5$ | $10^4$–$10^8$ | 25 |
| LFIA | UCNP-Ab | *Yersinia pestis*, *Burkholderia pseudomallei* | $10^5$ | $10^5$–$10^8$ | 26 |
| Luminescence assay | UCNP-Ab | *Escherichia coli* | 10 | 42–42×$10^6$ | 27 |
| Multiplexed luminescence assay | UCNP-Ab | *Escherichia coli*, *Staphylococcus aureus* | 47, 64 | $10^2$–$10^6$ | 28 |
| Multiplexed luminescence assay | UCNP-aptamer coupled with MNP-cDNA | *Staphylococcus aureus*, *Vibrio parahaemolyticus*, *Salmonella typhimurium* | 25, 10, 15 | 50–$10^6$ | 29 |
| FRET assay | UCNP-cDNA coupled with AuNP-aptamer | *Escherichia coli* | 3 | 5–$10^6$ | 30 |

BSA – bovine serum albumin; SA – streptavidin; LFIA – lateral-flow immunoassay; Ab – antibody; MNP – magnetic nanoparticle, AuNP – gold nanoparticle

[a] *E. coli* O157:H17, *Salmonella paratyphi* A, B, C, *Salmonella enteritidis*, *Salmonella typhi*, *Salmonella choleraesuis*, *Vibrio cholera* O1, O139, *Vibrio parahaemolyticus*

# References


1. J. D. Evans, R. S. Schwarz, Y. P. Chen, G. Budge, R. S. Cornman, P. De la Rua, J. R. de Miranda, S. Foret, L. Foster, L. Gauthier, E. Genersch, S. Gisder, A. Jarosch, R. Kucharski, D. Lopez, C. M. Lun, R. F. A. Moritz, R. Maleszka, I. Munoz and M. A. Pinto, *J. Apic. Res.*, 2013, **52**, 53.
2. D. M. Rissin, C. W. Kan, T. G. Campbell, S. C. Howes, D. R. Fournier, L. Song, T. Piech, P. P. Patel, L. Chang, A. J. Rivnak, E. P. Ferrell, J. D. Randall, G. K. Provuncher, D. R. Walt and D. C. Duffy, *Nat. Biotechnol.*, 2010, **28**, 595–599.
3. Z. Farka, T. Juřík, M. Pastucha and P. Skládal, *Anal. Chem.*, 2016, **88**, 11830-11836.
4. G. T. Hermanson, *Bioconjugate Techniques (Second Edition)*, Academic Press, New York, 2008.
5. D. Catty, *Antibodies volume II: A practical approach*, IRL Press, Oxford, 1989.
6. F. Wang, Y. Han, C. S. Lim, Y. H. Lu, J. Wang, J. Xu, H. Y. Chen, C. Zhang, M. H. Hong and X. G. Liu, *Nature*, 2010, **463**, 1061–1065.
7. A. Hlaváček, A. Sedlmeier, P. Skládal and H. H. Gorris, *ACS Appl. Mater. Interfaces*, 2014, **6**, 6930–6935.
8. A. Hlaváček, M. Peterek, Z. Farka, M. J. Mickert, L. Prechtl, D. Knopp and H. H. Gorris, *Microchim. Acta*, 2017, **184**, 4159–4165.
9. Z. Farka, M. J. Mickert, A. Hlaváček, P. Skládal and H. H. Gorris, *Anal. Chem.*, 2017, **89**, 11825–11830.
10. C. A. Schneider, W. S. Rasband and K. W. Eliceiri, *Nat. Methods*, 2012, **9**, 671-675.
11. D. E. Pinnock and N. E. Featherstone, *J. Apic. Res.*, 1984, **23**, 168–170.
12. V. Tomkies, J. Flint, G. Johnson, R. Waite, S. Wilkins, C. Danks, M. Watkins, A. G. S. Cuthbertson, E. Carpana, G. Marris, G. Budge and M. A. Brown, *Apidologie*, 2009, **40**, 63–72.
13. M. A. Z. Hornitzky and L. Smith, *J. Apic. Res.*, 1998, **37**, 293–294.
14. V. A. Govan, V. Brozel, M. H. Allsopp and S. Davison, *Appl. Environ. Microbiol.*, 1998, **64**, 1983–1985.
15. S. P. Djordjevic, K. Noone, L. Smith and M. A. Z. Hornitzky, *J. Apic. Res.*, 1998, **37**, 165–173.
16. B. A. McKee, S. P. Djordjevic, R. D. Goodman and M. A. Hornitzky, *Apidologie*, 2003, **34**, 19–27.
17. E. Forsgren, A. C. Lundhagen, A. Imdorf and I. Fries, *Microb. Ecol.*, 2005, **50**, 369–374.
18. A. Roetschi, H. Berthoud, R. Kuhn and A. Imdorf, *Apidologie*, 2008, **39**, 362–371.

19. G. E. Budge, B. Barrett, B. Jones, S. Pietravalle, G. Marris, P. Chantawannakul, R. Thwaites, J. Hall, A. G. S. Cuthbertson and M. A. Brown, *J. Invertebr. Pathol.*, 2010, **105**, 164–170.
20. R. Arai, T. Miyoshi-Akiyama, K. Okumura, Y. Morinaga, M. H. Wu, Y. Sugimura, M. Yoshiyama, M. Okura, T. Kirikae and D. Takamatsu, *J. Vet. Med. Sci.*, 2014, **76**, 491–498.
21. B. Dainat, D. Grossar, B. Ecoffey and C. Haldemann, *J. Microbiol. Methods*, 2018, **146**, 61–63.
22. M. Saleh, H. Soliman, H. Sorum, A. K. Fauske and M. El-Matbouli, *Vet. Rec.*, 2012, **171**, 400.
23. T. Erban, O. Ledvinka, M. Kamler, B. Hortova, M. Nesvorna, J. Tyl, D. Titera, M. Markovic and J. Hubert, *PeerJ*, 2017, **5**, 28.
24. P. Zhao, Y. Y. Wu, Y. H. Zhu, X. L. Yang, X. Jiang, J. F. Xiao, Y. X. Zhang and C. Z. Li, *Nanoscale*, 2014, **6**, 3804–3809.
25. Y. Zhao, H. R. Wang, P. P. Zhang, C. Y. Sun, X. C. Wang, X. R. Wang, R. F. Yang, C. B. Wang and L. Zhou, *Sci. Rep.*, 2016, **6**, 8.
26. Z. Q. Liang, X. C. Wang, W. Zhu, P. P. Zhang, Y. X. Yang, C. Y. Sun, J. J. Zhang, X. R. Wang, Z. Xu, Y. Zhao, R. F. Yang, S. L. Zhao and L. Zhou, *ACS Appl. Mater. Interfaces*, 2017, **9**, 3497–3504.
27. W. X. Pan, J. W. Zhao and Q. S. Chen, *J. Agric. Food Chem.*, 2015, **63**, 8068–8074.
28. B. Zhang, H. H. Li, W. X. Pan, Q. S. Chen, Q. Ouyang and J. W. Zhao, *Food Anal. Methods*, 2017, **10**, 2036–2045.
29. S. J. Wu, N. Duan, Z. Shi, C. C. Fang and Z. P. Wang, *Anal. Chem.*, 2014, **86**, 3100–3107.
30. B. R. Jin, S. R. Wang, M. Lin, Y. Jin, S. J. Zhang, X. Y. Cui, Y. Gong, A. Li, F. Xu and T. J. Lu, *Biosens. Bioelectron.*, 2017, **90**, 525–533.